

MRZ code extraction from visa and passport documents using convolutional neural networks

Yichuan Liu, Hailey James, Otkrist Gupta, Dan Raviv

¹Lendbuzz
125 High St Suite 2512
Boston, MA 02110
yichuan.liu@lendbuzz.com

Abstract

Detecting and extracting information from Machine-Readable Zone (MRZ) on passports and visas is becoming increasingly important for verifying document authenticity. However, computer vision methods for performing similar tasks, such as optical character recognition (OCR), fail to extract the MRZ given digital images of passports with reasonable accuracy. We present a specially designed model based on convolutional neural networks that is able to successfully extract MRZ information from digital images of passports of arbitrary orientation and size. Our model achieved 100% MRZ detection rate and 98.36% character recognition macro-f1 score on a passport and visa dataset.

Introduction

In domains such as finance, immigration, and administration, digital copies of passports are playing an increasingly important role in identity and information verification. However, automatic information retrieval from passports and visas can be difficult due to non-uniform passport and visa layouts. Information such as the name, birth date, expiration date, and issue date appear in a variety of formats and locations on passports and visas from different issuing authorities. Additionally, unlike physical passports and visas which can be examined for authenticity, digital copies of these documents present a lower barrier to forgery and manipulation. Simple image editing software can be used to alter key details on the passport or visa for purposes of fraud.

The Machine-Readable Zone (MRZ) on passports and visas is critical for combating both of these challenges. For purposes of information retrieval, the MRZ presents key information in a pre-specified format and location. Similarly, the format of the MRZ makes it more difficult to manipulate than the rest of the passport, requiring domain knowledge and greater attention to detail. Locating and extracting passport and visa MRZ thus presents an important and unique challenge in computer vision.

We propose a novel neural network model designed specifically for handling MRZ text, with characteristics designed to overcome the challenges unique to MRZ extraction. Specifically, our architecture backbone is inspired by

EAST (Zhou et al. 2017), a scene text detector, with atrous spatial pyramid pooling layers to handle images with varying sizes and added a recognition branch to detect and extract the 88 characters long MRZ text. For better handling passport images with various sizes, we proposed a novel sequential two-model system, in which the first "course" model extracts the MRZ bounding box and the second "fine" model refines bounding box prediction and extracts the text from the MRZ. This system design offers the additional benefit of decreasing the memory and time required for detection. Combined, this design results in 100% MRZ detection rate and 98.36% character recognition macro-f1 score on digital images of passports and visas.

Background

Machine-Readable Zone (MRZ)

The Machine-Readable Zone (MRZ) appears on passports and visas of most countries to facilitate robust data extraction and processing. Because passports from different states vary in script, style, and format, the MRZ provides a simple way to extract key details from the passport, including the name, passport number, nationality, date of birth, sex, and passport expiration date. Generally appearing near the beginning of the passport on the identity page, the MRZ appears as two lines of 44 characters long text on the bottom of the page. The MRZ consists only of the Arabic numerals (digits 0-9), the capital letters of the Latin alphabet ('A', 'B', 'C', ...), and the filler character '<'. While historically used for quickly extracting the important information from a variety of passports, the MRZ is becoming useful for document verification and manipulation detection. For example, businesses and states can verify that the information encoded in the MRZ matches the information in the visual zone (VZ) of the passport. While highly-motivated and skilled forgers can additionally alter the MRZ, validation of the MRZ information is a simple, low-cost method for detecting basic manipulations, such as name, expiration, or birth date changes. As photographs of passports gain popularity as a method for verifying identity, accurately and quickly extracting the passport MRZ becomes an essential part of the identity verification pipeline.



Figure 1: Example passport images. Passport can either occupy only a small part of the image (a) or span the whole image (b).

Related Work

Models leveraging advances in deep learning, such as convolutional neural networks (CNNs), have been successfully employed in similar tasks, such as determining the region of interest (ROI) of a photograph (Long, Shelhamer, and Darrell 2015; Ren et al. 2015) and optical character recognition (OCR) (Wang and Hu 2017). Among these, MRZ extraction from digital passport images is most related to work in detecting and extracting text in natural scenes.

Text Detection in Natural Scenes

Several techniques in computer vision have been developed or leveraged for improved performance in text scene detection. (Liu and Sarkar) and (Zhu et al. 2007) use image binarization to segment text regions. (Merino-Gracia, Lenc, and Mirmehdi 2012) (Donoser, Arth, and Bischof 2007) and (González, Bergasa, and Yebes 2012) use Maximally Stable Extremal Region (MSER) to improve detection. (Fabrizio, Marcotegui, and Cord 2009) and (Minetto et al. 2011) use morphological operations to segment text regions. (Mishra, Alahari, and Jawahar 2012) and (Pan, Hou, and Liu 2011) use Histogram of Oriented Gradients (HOG) for improved performance. (Kasar and Ramakrishnan 2012) and (Neumann and Matas 2012) use color properties to both detect and extract text regions.

More recently, the ICDAR 2015 Robust Reading Competition dataset has provided a valuable benchmark for scene text detection and extraction (Karatzas et al. 2015). Many recent works demonstrate impressive performance on this dataset. (Zhang et al. 2016) use Fully Convolutional Network (FCN) models, trained separately to predict the saliency map of the text regions and the centroid of each character. (Shi, Bai, and Belongie 2017) similarly train an FCN, but on the segments and links of the text which are combined for final detections. (He et al. 2017) propose a single shot attention-based mechanism that attempts a coarse to fine approach to text detection. (Hu et al. 2017) leverage a weakly supervised framework that uses word annotations to train the character detector. (Zhou et al. 2017) propose EAST (An Efficient and Accurate Scene Text Detector), which skips intermediate steps like candidate aggregation and word partitioning to directly predict words and text lines. (Long et al. 2018) attempts to consider more free-form text examples such as curved text using a FCN to estimate geometric attributes of the scene regions. (Liao, Shi, and Bai 2018) iterate on the object detector method proposed in (Liu

et al. 2016). (Deng et al. 2018) propose a novel method for scene text detection using instance segmentation. (Lyu et al. 2018c) and (Deng et al. 2019) leverage the corner points of the text bounding boxes for better segmentation and detection. (Wang et al. 2019) generate different kernel scales for each text instance in order to split close text instances. (Dai et al. 2018) combine multi-level features during feature extraction for improved performance. Several recent papers leverage pyramid attention or pyramid pooling (Dai et al. 2018; Xie et al. 2018; Liu et al. 2019). (Lyu et al. 2018a) improves performance with an architecture inspired by Mask R-CNN (He et al. 2018a). (Liao et al. 2019) propose a module to perform binarization in a segmentation network. (Liu et al. 2018a) trains a network for simultaneous detection and recognition by sharing convolutional features between the two processes. (Xu et al. 2019) leverage multiple branches to achieve geometry normalization. (Liu et al. 2020) build on previous work and incorporate a method to discretize the potential quadrilaterals into various horizontal and vertical positions. So far, (Xing et al. 2019) achieve the most impressive performance by training on synthetic data, using characters as the basic element, and eliminating ROI pooling.

Passport MRZ Detection and Extraction

While Optical Character Recognition (OCR) software may extract text with reasonably good accuracy, state of the art methods struggle to accurately extract MRZ text. This is evidenced by the relatively poor MRZ detection rate of PassportEye (Tretyakov 2016) which is based on Tesseract OCR (Smith 2007). Similarly, models designed for scene text extraction are not naturally well-suited for MRZ extraction. For example, end-to-end scene text recognition models such as FOTS (Liu et al. 2018b) and Mask Textspotter (Lyu et al. 2018b) may be able to detect and recognize MRZ. However, these models are designed to handle text lines with arbitrary number of characters and employed techniques such as LSTM (Hochreiter and Schmidhuber 1997) to recognize text. Since MRZ text is always 2 lines, 44 characters per line, a specifically designed neural network architecture can help boosting text recognition performance. Additional, typical passport images used for identity verification purposes are taken with a smartphone, resulting in a high resolution images in which the passport appears in various places and at various sizes (see Figure 1), presenting an additional challenge.

In 2011, (Bessmeltsev, Bulushev, and Goloshevsky 2011) presented a hardware-based method for portable passport readers for detecting and reading the MRZ of physical passports. (Lee and Kwak 2015) propose a method for extracting the passport MRZ using template matching, but only for images in which the passport is surrounded by a black border. (Chernyshova et al. 2019) explored optical font recognition for forgery detection in passport MRZs. (Petrova and Bulatov 2019) discuss methods for correcting or post-processing passport MRZ recognition results. (Hartl, Arth, and Schmalstieg 2015) present an algorithm for reading MRZ images on mobile devices, achieving an MRZ detection rate of 88.18% with 5 frames and 56.1% with single frame, along with a character reading rate of 98.58%. In comparison our model

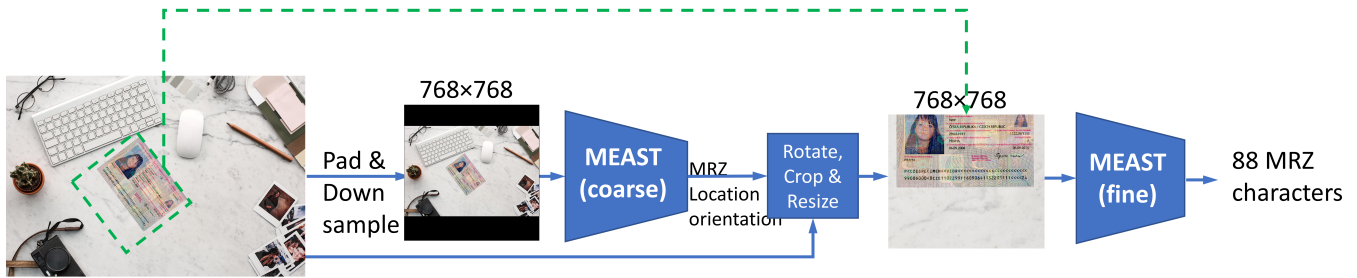


Figure 2: Overall structure of MRZNet. MEAST (coarse) roughly locate the MRZ region from a down-sampled image whereas MEAST (fine) refine the localization on the original high resolution image and recognize the MRZ text.

boasts a 100% single frame MRZ detection rate and 98.36% character recognition macro-f1 score on passport and visa images.

Methodology

MRZNet is a framework that detects and recognizes the MRZ code of passport and visa images of arbitrary orientation and sizes. This section describes the details of the architecture of MRZNet.

Overall architecture

The overall architecture of MRZNet is illustrated in Figure 2. It includes two neural networks, MEAST (coarse) and MEAST (fine), which share similar architectures. The high resolution original image is first padded to be a square and then down-samples to 768 x 768 as input to MEAST (coarse). MEAST (coarse) localizes the MRZ region and output the bounding box location and orientation. We then rotate the original image to make it upright, crop the image centered at the bounding box center and pad/resize the image accordingly to obtain a 768 x 768 image in which the MRZ region is roughly placed in the center and span the whole image. This image is then feed into MEAST (fine) for finer localization and MRZ code recognition. We adopt this architecture for handling passport/visa images of arbitrary orientation and sizes. A real world passport/visa image, whether it is scanned or taken from a smart phone, are usually of high resolutions. Depending on how the user captures the image, the MRZ region can either be occupying only a small region of the image (Figure 1(a)) or it may span the whole image (Figure 1 (b)). Feeding the high resolution image directly into a neural network is not only time and memory consuming but may result in poor MRZ code recognition results for images like Figure 1 (b) because localizing these high resolution images require the neural network to have very large receptive field. On the other hand, feeding a down-sampled image to a neural network will result in poor MRZ recognition results for images like Figure 1 (a) because the text will be unrecognizable in low resolution. It is for solving this dilemma that we adopt an architecture that first roughly localizes the MRZ region using a down-sampled the image, and then standardizes the images to Figure 1 (b) cases and finally perform MRZ code recognition.

MRZ-EAST

Inspired by EAST (Zhou et al. 2017), we propose MRZ-EAST (MEAST), an end-to-end trainable neural network for MRZ localization and recognition. The architecture of MEAST is shown in Figure 3. We adopt MobileNetV2 (Sandler et al. 2018) as the backbone. Similar to EAST, we concatenate up-sampled high-level semantic feature map with low-level feature map and merge them gradually in a U-shaped architecture. This way the neural network utilizes the feature from different levels and will able to detect MRZ regions of different sizes. However, since EAST was proposed for detecting text in natural scenes and in natural scenes, its not designed for cases when a line of text will spans the whole image (see Figure 1 (b)). For handling these images, a larger receptive field is required to look at the “big picture” of the image in order to accurately detect the large text bounding box. We applied atrous spatial pyramid pooling (ASPP) at the end of the MobileNetV2 feature extractor to allow for bigger receptive fields. ASPP have been previously adopted by (Sermanet et al. 2013), (Giusti et al. 2013), (Simonyan and Zisserman 2014) and (Chen et al. 2018) for field-of-view enlargement. To further increase the field-of-view, we stacked multiple layers of ASPP in the fashion of a ResNet (He et al. 2016). After feature-merging, 1x1 convolutional layers is applied for output the likelihood of a MRZ region present in the pixel (the score map), the location of MRZ text boxes (4 channels, distance of the pixel locations to the top, right, bottom and left boundaries of the rectangle, respectively) and the MRZ box rotation angle. The non-maximum suppression algorithm is applied to select the most probable MRZ bounding box. Finally, a recognition branch is applied given the MRZ bounding box and convolutional output map of feature-merging branch to extract the MRZ text.

MRZ-EAST pipeline

We first extract feature maps from a passport/visa image using MobileNetV2 backbone. At the end of the stage 4 convolutional layers, MobileNetV2 produces 320 feature maps of 24×24 sizes. We then add four convolutional layers that running in parallel to form a ASPP layer. These four convolutional layers have a dilation rate (Chen et al. 2018) of 1, 2, 4 and 8 respectively. We concatenate the feature maps pro-

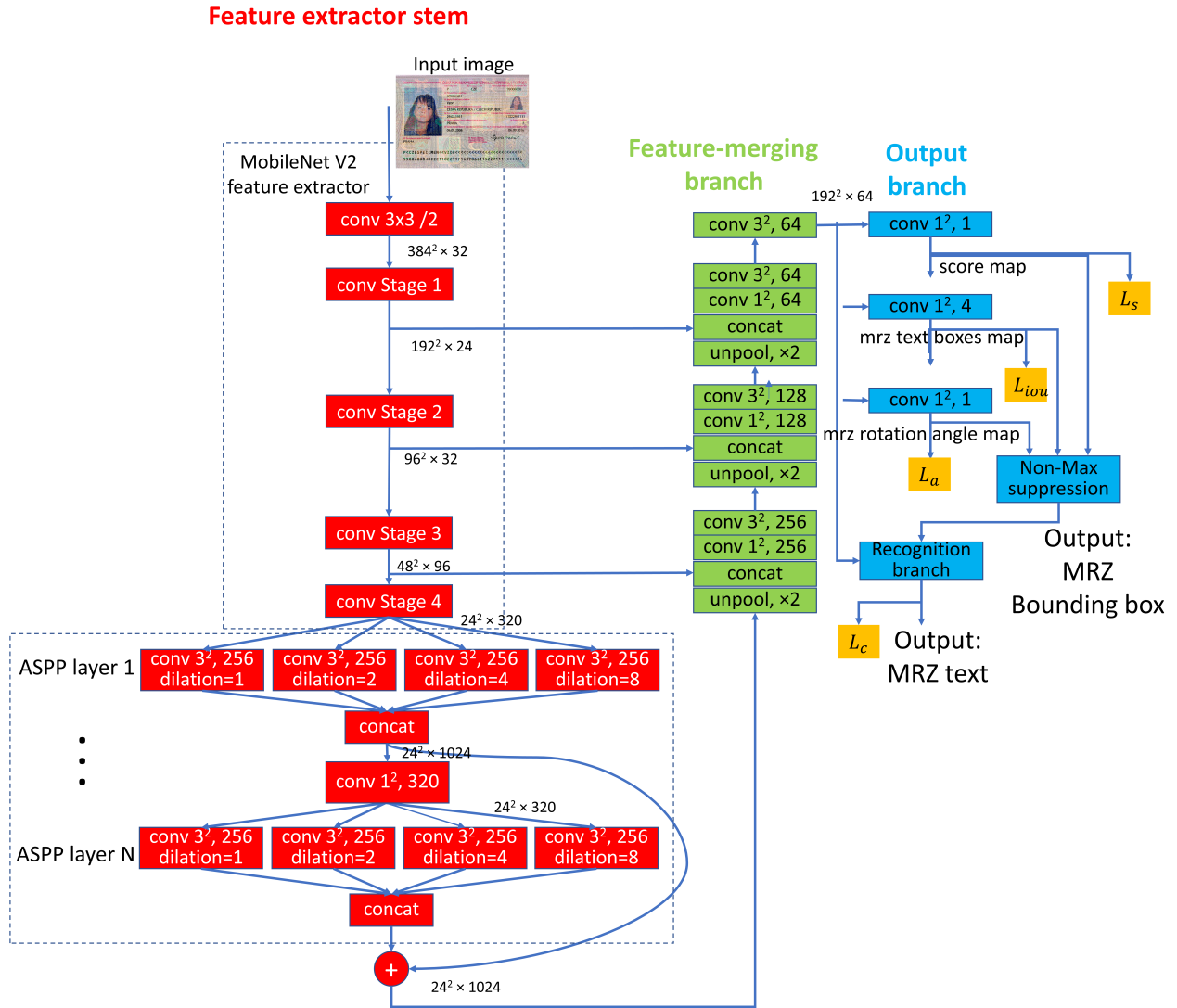


Figure 3: MRZ-EAST (MEAST) with N atrous spatial pyramid pooling (ASPP) layers. Both MEAST (coarse) and MEAST (fine) used the same architecture and loss as shown in this figure but with different parameter N . We modified EAST by adopting MobileNet V2 as backbone, stacking N ASPP layers on top of the last convolutional stage to increase the receptive field and adding a text recognition branch in addition to text localization branch.

duced by these four layers (the concatenation layer) and then applied a 1×1 convolutional layer to reduce the number of feature maps to be 320 before feeding the resulting feature maps to the next ASPP layer. Shortcuts were added between the concatenation layer of two ASPP layers. After N ASPP layers, we bilinearly upsampled (unpool) the feature maps to 48×48 sizes before concatenate them with the feature maps output from the end of stage 3 convolutional layer of MobileNetV2. A 1×1 followed by a 3×3 convolutional layer is used to fuse these feature maps. We then bilinearly upsampled the resulting feature maps to 96×96 sizes and concatenate them with output of the stage 2 convolutional layers of MobileNetV2. After fuse the feature maps with 2 convolutional layers, we bilinearly upsampled them to 192×192 sizes and concatenate them with the output of stage 1 convolutional layers of MobileNet V2. Three convolutional layers are then applied to fuse and extract features from these feature maps to produce the output of feature-merging branch, which is composed of 64 feature maps of 192×192 sizes. For each pixel in the output of feature-merging branch, we apply 1×1 convolutional layers at the output branch to produce a 0-1 probability score indicate the presence of MRZ (the score map) at the pixel, the distance from the top, bottom, left and right of the mrz bounding box to the pixel (mrz text box map) and the rotating angle of the bounding box (mrz rotation angle map). Because we have 192×192 pixels, a total of $192 \times 192 = 36864$ bounding boxes are produced as a result. We reject those bounding boxes that have a probability score lower than 0.5 and used non-max suppression (NMS) to fuse the rest of bounding boxes. The bound box that has the highest score is than selected as input to the recognition branch.

Recognition branch

Both the MEAST (coarse) and MEAST (fine) includes a recognition branch for recognizing MRZ text. Our recognition branch is inspired from (He et al. 2018b). Figure 4 shows the architecture. Given the quadrilateral MRZ region from NMS, we sample a 16 by 352 grid from the convolutional map at the output of feature-merging branch. The same as (He et al. 2018b), we used bilinear sampling. More specifically, the feature vector v_p of a sampling point p at spatial location (p_x, p_y) , is calculated as follows:

$$v_p = \sum_{i=0}^3 v_{pi} g(p_x, p_{ix}) g(p_y, p_{iy}) \quad (1)$$

where v_{pi} refer to the surrounding four points of point p and $g(p_1, p_2)$ is the bilinear interpolation function.

After extracting the sampling grid, three layers of 3×3 convolution and 2×2 max-pooling is applied to down-sample the extracted feature map from 16×352 (points by points) to 2×44 (lines by characters per line). We doubled the number of channels with each down-sampling. Finally, a 1×1 convolutional layer is applied to reduce the number of channels to 37 (the number of valid characters in MRZ code) and soft-max is applied to obtain the probability of occurrence for each of the 88 characters.

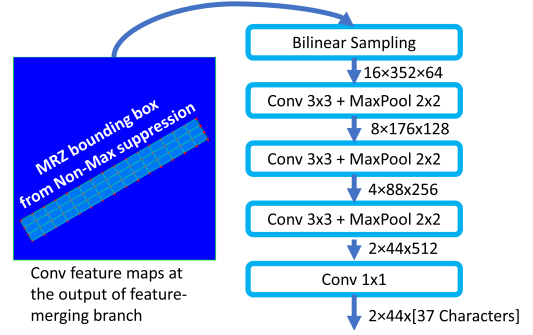


Figure 4: Architecture of the recognition branch. Instead of adopting LSTM for recognizing arbitrary length text as in typical scene text recognition networks, we bilinearly sample a 16 by 352 grid points from the output convolutional layer of EAST and pass it through several full convolutional layers and max pooling layers to reduce the feature map size to 2 by 44 for recognizing the 2 lines, 44 characters per line MRZ text.

Loss functions

MEAST(coarse) and MEAST(fine) are trained separately with the same loss function as follows:

$$L = L_s + \lambda_g L_g + \lambda_c L_c \quad (2)$$

where L_s is the loss for score map, L_g is the loss for geometry, L_c is the loss for character classification. In our experiment, we set λ_g and λ_c to be 1. For the loss of score map, we used dice loss:

$$L_s = 1 - \frac{2 \sum_x s_x s_x^*}{\sum_x s_x + \sum_x s_x^*} \quad (3)$$

where s_x and s_x^* are predicted score and ground truth score, respectively. For the geometry loss, we adopt the intersection over union (IoU) loss and rotation angle loss as in EAST (Zhou et al. 2017):

$$L_g = L_{iou} + \lambda_a L_a \quad (4)$$

$$L_{iou} = \frac{1}{\Omega} \sum_{x \in \Omega} IoU(R_x, R_x^*) \quad (5)$$

$$L_a = (1 - \cos(\theta_x, \theta_x^*)) \quad (6)$$

where R_x , R_x^* , θ_x and θ_x^* are predicted bounding box, ground truth bounding box, predicted orientation and ground truth orientation, respectively. IoU is calculated as follows:

$$IoU(R_x, R_x^*) = \frac{R_x \cap R_x^*}{R_x \cup R_x^*} \quad (7)$$

In our experiment, the weight λ_a is set to 10. For the character classification loss, we used the cross-entropy loss:

$$L_c = \sum_{i=0}^c y_i \log(f_i(x)) \quad (8)$$

where c is the number of possible different characters, $f_i(x)$ is the network output of class i for image sample x , y_i is the one hot ground truth label.

Implementation details

For the MobileNetV2 backbone, we loaded weights pre-trained on the ImageNet dataset (Deng et al. 2009) before finetuning on our MRZ dataset. For training MEAST (coarse), we augmented the dataset by randomly rotating the images in the range of $[-180^\circ, 180^\circ]$ and randomly padding with black borders so that the new image height is in the range of 1-2 times the height of the original image or crop image with random sizes as long as the MRZ region is intact. For training MEAST (fine), we augmented the dataset by randomly rotate the image in the range of $[-20^\circ, 20^\circ]$ respect to the upright position (the image was first rotated so that the MRZ region is upright before random rotation). We found that it is important to make sure that the rotation angle is small for MEAST (fine). We then crop the image so that the cropped region is a square and the MRZ region is roughly placed in the center of the image with the left and right borders randomly selected to be 0.05-0.25 times the width of the MRZ region. For both MEAST (coarse) and MEAST (fine), we trained the model for 120 epochs with Adam optimizer (Kingma and Ba 2014) and a initial learning rate of 0.0001, $\beta_1 = 0.9$ and $\beta_2 = 0.999$. The learning rate was decreased by a factor of 10 at 60 epochs. The batch size is selected to be 6. Models are trained with a single GeForce RTX 2070 graphic card. The time used to train both MEAST (coarse) and MEAST (fine) are approximately 1 day, making it a total of 2 days to train the entire model.

Experimental evaluation

In this section, we evaluate the performance of MRZNet with experiments. We also report results from ablation studies to verify the effectiveness of the design choices.

Dataset

We evaluated our algorithm on a dataset consist of 4820 passport/visa images. These real world images are either scanned by a scanner or taken from a smart phone and uploaded to our database. Each of these images contains a single passport or visa. We manually annotated the ground truth bounding box and MRZ text for all images. We used 70% (3374) for training, 15% (723) for validation and 15% (723) for testing.

Comparison with existing solution

We compared our MRZNet against existing MRZ recognition solutions MRZ-detection (Kostro and Zasso 2020), PassportEye (Tretyakov 2016) which is based on Tesseract OCR (Smith 2007), the UltimateMRZ (doubango.org 2020), a deep learning based commercial solution and the algorithm proposed by Hartl et al. (Hartl, Arth, and Schmalstieg 2015). It can be seen from Table 1 that our MRZNet outperforms MRZ-detection, the OCR based PassportEye and deep learning based UltimateMRZ by a large margin. Hartl et al. (Hartl, Arth, and Schmalstieg 2015) achieved character recognition rate of 98.6%. Their MRZ detection rate, however, is only 56.1% (single frame) and 88.2% rate (5 frames) whereas our single frame MRZ detection rate is 100%.

Table 1: MRZ detection and character recognition (in macro-f1 score) results on the test set for MRZNet and other solutions

Method	MRZ Detection	Character Recog.
PassportEye	45.29%	45.24%
MRZ-detection	77.18%	35.93%
UltimateMRZ ^a	69.11%	84.47%
Hartl2014 ^b	56.1%	98.60%
MRZNet	100.00%	98.36%

^aRecognition rate are based on an average of 76 out of 88 characters available in the free version

^bSingle frame results from their dataset reported by the paper; Recognition result reported is accuracy not F1-score

Table 2: Results on validation set from MEAST (coarse). We show the variation of bounding box detection IOU and MRZ text recognition macro F1-score with different number of ASPP layers

Num. of ASPP	IoU	Macro F1-score
0	0.8701	56.56%
1	0.8508	67.87%

Ablation Study

We performed ablation study to evaluate the effectiveness of the two stage model and the added ASPP layers and the results are shown in Table 2 and Table 3. From Table 1, it can be seen that using only MEAST (coarse) will result in poor MRZ text recognition accuracy (with 67.87% macro f1-score as the best result). Including a single ASPP layer to MEAST (coarse) improved the MRZ text recognition performance from 56.56% to 67.87%. However, the bounding box localization accuracy decreased from 0.8701 to 0.8508 IoU. Considering the objective of MEAST (coarse) is localization, we haven't included any ASPP layers in the final model for MEAST (coarse). From Table 3, it can be seen that the MRZ recognition accuracy is much improved by using MEAST (fine) after MEAST (coarse). Including one single layer of ASPP improved the MRZ text recognition accuracy from 98.40% to 98.91%. By stacking 3 ASPP layers, the accuracy further improved to 99.21%. These results demonstrated the effectiveness of proposed two stage model and the ASPP layers.

Conclusion

In this work, we presented MRZNet, a framework specifically designed for localizing and recognizing the MRZ text in passport and visa images. A novel two stage model process is adopted so that MRZNet can handle passport/visa images of varies sizes from high resolution images. We modified EAST (Zhou et al. 2017), a scene text detector, with a recognition branch for recognizing MRZ text. By stacking multiple layers of ASPP, we increased the receptive field of the model and improved the MRZ text recognition accu-

Table 3: Results on validation set from MEAST (fine). We show the variation of bounding box detection IOU and MRZ text recognition macro F1-score with different number of ASPP layers

Num. of ASPP	IoU	Macro F1-score
0	0.9071	98.40%
1	0.9059	98.91%
3	0.9144	99.21%

racy. Experiment evaluation demonstrated the effectiveness of our approach. Possible future research include: 1) add a dewarp component to the framework to make the pipeline works even for passport images that are warped and the text lines are hence curved; 2) modify the architecture for single character level bounding box detection and recognition for further improving the robustness of the pipeline.

References

- Bessmeltsev, V.; Bulushev, E.; and Goloshevsky, N. 2011. High-speed OCR algorithm for portable passport readers. *21st International Conference on Computer Graphics and Vision, GraphiCon'2011 - Conference Proceedings*.
- Chen, L.-C.; Papandreou, G.; Kokkinos, I.; Murphy, K.; and Yuille, A. L. 2018. DeepLab: Semantic Image Segmentation with Deep Convolutional Nets, Atrous Convolution, and Fully Connected CRFs. *IEEE Transactions on Pattern Analysis and Machine Intelligence* 40(4): 834848. ISSN 2160-9292. doi:10.1109/tpami.2017.2699184. URL <http://dx.doi.org/10.1109/TPAMI.2017.2699184>.
- Chernyshova, Y. S.; Aliev, M. A.; Gushchanskaia, E. S.; and Sheshkus, A. V. 2019. Optical Font Recognition in Smartphone-Captured Images, and its Applicability for ID Forgery Detection. *Eleventh International Conference on Machine Vision (ICMV 2018)* 59. doi:10.1117/12.2522955. URL <http://arxiv.org/abs/1810.08016>. ArXiv: 1810.08016.
- Dai, Y.; Huang, Z.; Gao, Y.; Xu, Y.; Chen, K.; Guo, J.; and Qiu, W. 2018. Fused Text Segmentation Networks for Multi-oriented Scene Text Detection. *arXiv:1709.03272 [cs]* URL <http://arxiv.org/abs/1709.03272>. ArXiv: 1709.03272.
- Deng, D.; Liu, H.; Li, X.; and Cai, D. 2018. PixelLink: Detecting Scene Text via Instance Segmentation. *arXiv:1801.01315 [cs]* URL <http://arxiv.org/abs/1801.01315>. ArXiv: 1801.01315.
- Deng, J.; Dong, W.; Socher, R.; Li, L.; Kai Li; and Li Fei-Fei. 2009. ImageNet: A large-scale hierarchical image database. In *2009 IEEE Conference on Computer Vision and Pattern Recognition*, 248–255.
- Deng, L.; Gong, Y.; Lin, Y.; Shuai, J.; Tu, X.; Zhang, Y.; Ma, Z.; and Xie, M. 2019. Detecting Multi-Oriented Text with Corner-based Region Proposals. *Neurocomputing* 334: 134–142. ISSN 09252312. doi:10.1016/j.neucom.2019.01.013. URL <http://arxiv.org/abs/1804.02690>. ArXiv: 1804.02690.
- Donoser, M.; Arth, C.; and Bischof, H. 2007. Detecting, Tracking and Recognizing License Plates. In Yagi, Y.; Kang, S. B.; Kweon, I. S.; and Zha, H., eds., *Computer Vision ACCV 2007*, Lecture Notes in Computer Science, 447–456. Berlin, Heidelberg: Springer. ISBN 978-3-540-76390-1. doi:10.1007/978-3-540-76390-1_44.
- doubango.org. 2020. URL <https://github.com/DoubangoTelecom/ultimateMRZ-SDK#Getting-started-Adding-the-SDK-to-your-project>.
- Fabrizio, J.; Marcotegui, B.; and Cord, M. 2009. Text segmentation in natural scenes using Toggle-Mapping. In *2009 16th IEEE International Conference on Image Processing (ICIP)*, 2373–2376.
- Giusti, A.; Ciresan, D. C.; Masci, J.; Gambardella, L. M.; and Schmidhuber, J. 2013. Fast image scanning with deep max-pooling convolutional neural networks. *2013 IEEE International Conference on Image Processing* doi:10.1109/icip.2013.6738831. URL <http://dx.doi.org/10.1109/ICIP.2013.6738831>.
- González, Á.; Bergasa, L. M.; and Yebes, J. J. 2012. Location in Complex Images.
- Hartl, A.; Arth, C.; and Schmalstieg, D. 2015. Real-time Detection and Recognition of Machine-Readable Zones with Mobile Devices. In *Proceedings of the 10th International Conference on Computer Vision Theory and Applications*, 79–87. Berlin, Germany: SCITEPRESS - Science and Technology Publications. ISBN 978-989-758-089-5 978-989-758-090-1 978-989-758-091-8.
- He, K.; Gkioxari, G.; Dollr, P.; and Girshick, R. 2018a. Mask R-CNN. *arXiv:1703.06870 [cs]* URL <http://arxiv.org/abs/1703.06870>. ArXiv: 1703.06870.
- He, K.; Zhang, X.; Ren, S.; and Sun, J. 2016. Deep Residual Learning for Image Recognition. *2016 IEEE Conference on Computer Vision and Pattern Recognition (CVPR)* doi:10.1109/cvpr.2016.90. URL <http://dx.doi.org/10.1109/cvpr.2016.90>.
- He, P.; Huang, W.; He, T.; Zhu, Q.; Qiao, Y.; and Li, X. 2017. Single Shot Text Detector with Regional Attention. *arXiv:1709.00138 [cs]* URL <http://arxiv.org/abs/1709.00138>. ArXiv: 1709.00138.
- He, T.; Tian, Z.; Huang, W.; Shen, C.; Qiao, Y.; and Sun, C. 2018b. An End-to-End TextSpotter with Explicit Alignment and Attention. *2018 IEEE/CVF Conference on Computer Vision and Pattern Recognition* doi:10.1109/cvpr.2018.00527. URL <http://dx.doi.org/10.1109/CVPR.2018.00527>.
- Hochreiter, S.; and Schmidhuber, J. 1997. Long short-term memory. *Neural computation* 9(8): 1735–1780.
- Hu, H.; Zhang, C.; Luo, Y.; Wang, Y.; Han, J.; and Ding, E. 2017. WordSup: Exploiting Word Annotations for Character based Text Detection. *arXiv:1708.06720 [cs]* URL <http://arxiv.org/abs/1708.06720>. ArXiv: 1708.06720.
- Karatzas, D.; Gomez-Bigorda, L.; Nicolaou, A.; Ghosh, S.; Bagdanov, A.; Iwamura, M.; Matas, J.; Neumann, L.; Chandrasekhar, V. R.; Lu, S.; Shafait, F.; Uchida, S.; and Valveny, E. 2015. ICDAR 2015 competition on Robust Reading. In *13th IAPR International Conference on Document Analysis and Recognition, ICDAR 2015 - Conference Proceedings*,

- 1156–1160. IEEE Computer Society. doi:10.1109/ICDAR.2015.7333942. URL <https://kyushu-u.pure.elsevier.com/en/publications/icdar-2015-competition-on-robust-reading>.
- Kasar, T.; and Ramakrishnan, A. 2012. Multi-script and Multi-oriented Text Localization from Scene Images. volume 7139, 1–14. ISBN 978-3-642-29364-1. doi:10.1007/978-3-642-29364-1_1.
- Kingma, D. P.; and Ba, J. 2014. Adam: A Method for Stochastic Optimization.
- Kostro, D.; and Zasso, M. 2020. URL <https://github.com/image-js/mrz-detection>.
- Lee, H.; and Kwak, N. 2015. Character recognition for the machine reader zone of electronic identity cards. In *2015 IEEE International Conference on Image Processing (ICIP)*, 387–391. doi:10.1109/ICIP.2015.7350826.
- Liao, M.; Shi, B.; and Bai, X. 2018. TextBoxes++: A Single-Shot Oriented Scene Text Detector. *IEEE Transactions on Image Processing* 27(8): 3676–3690. ISSN 1057-7149, 1941-0042. doi:10.1109/TIP.2018.2825107. URL <http://arxiv.org/abs/1801.02765>. ArXiv: 1801.02765.
- Liao, M.; Wan, Z.; Yao, C.; Chen, K.; and Bai, X. 2019. Real-time Scene Text Detection with Differentiable Binarization. *arXiv:1911.08947 [cs]* URL <http://arxiv.org/abs/1911.08947>. ArXiv: 1911.08947.
- Liu, J.; Liu, X.; Sheng, J.; Liang, D.; Li, X.; and Liu, Q. 2019. Pyramid Mask Text Detector. *arXiv:1903.11800 [cs]* URL <http://arxiv.org/abs/1903.11800>. ArXiv: 1903.11800.
- Liu, W.; Anguelov, D.; Erhan, D.; Szegedy, C.; Reed, S.; Fu, C.-Y.; and Berg, A. C. 2016. SSD: Single Shot MultiBox Detector. *Lecture Notes in Computer Science* 2137. ISSN 1611-3349. doi:10.1007/978-3-319-46448-0_2. URL http://dx.doi.org/10.1007/978-3-319-46448-0_2.
- Liu, X.; Liang, D.; Yan, S.; Chen, D.; Qiao, Y.; and Yan, J. 2018a. FOTS: Fast Oriented Text Spotting with a Unified Network. *arXiv:1801.01671 [cs]* URL <http://arxiv.org/abs/1801.01671>. ArXiv: 1801.01671.
- Liu, X.; Liang, D.; Yan, S.; Chen, D.; Qiao, Y.; and Yan, J. 2018b. Fots: Fast oriented text spotting with a unified network. In *Proceedings of the IEEE conference on computer vision and pattern recognition*, 5676–5685.
- Liu, Y.; He, T.; Chen, H.; Wang, X.; Luo, C.; Zhang, S.; Shen, C.; and Jin, L. 2020. Exploring the Capacity of an Orderless Box Discretization Network for Multi-orientation Scene Text Detection. *arXiv:1912.09629 [cs]* URL <http://arxiv.org/abs/1912.09629>. ArXiv: 1912.09629.
- Liu, Z.; and Sarkar, S. ????. *Robust Outdoor Text Detection Using Text Intensity and Shape Features*.
- Long, J.; Shelhamer, E.; and Darrell, T. 2015. Fully convolutional networks for semantic segmentation. In *Proceedings of the IEEE conference on computer vision and pattern recognition*, 3431–3440.
- Long, S.; Ruan, J.; Zhang, W.; He, X.; Wu, W.; and Yao, C. 2018. TextSnake: A Flexible Representation for Detecting Text of Arbitrary Shapes. *arXiv:1807.01544 [cs]* URL <http://arxiv.org/abs/1807.01544>. ArXiv: 1807.01544.
- Lyu, P.; Liao, M.; Yao, C.; Wu, W.; and Bai, X. 2018a. Mask TextSpotter: An End-to-End Trainable Neural Network for Spotting Text with Arbitrary Shapes. *arXiv:1807.02242 [cs]* URL <http://arxiv.org/abs/1807.02242>. ArXiv: 1807.02242.
- Lyu, P.; Liao, M.; Yao, C.; Wu, W.; and Bai, X. 2018b. Mask textspotter: An end-to-end trainable neural network for spotting text with arbitrary shapes. In *Proceedings of the European Conference on Computer Vision (ECCV)*, 67–83.
- Lyu, P.; Yao, C.; Wu, W.; Yan, S.; and Bai, X. 2018c. Multi-Oriented Scene Text Detection via Corner Localization and Region Segmentation. *arXiv:1802.08948 [cs]* URL <http://arxiv.org/abs/1802.08948>. ArXiv: 1802.08948.
- Merino-Gracia, C.; Lenc, K.; and Mirmehdi, M. 2012. A Head-Mounted Device for Recognizing Text in Natural Scenes. In Iwamura, M.; and Shafait, F., eds., *Camera-Based Document Analysis and Recognition*, Lecture Notes in Computer Science, 29–41. Berlin, Heidelberg: Springer. ISBN 978-3-642-29364-1. doi:10.1007/978-3-642-29364-1_3.
- Minetto, R.; Thome, N.; Cord, M.; Stolfi, J.; Precioso, F.; Guyomard, J.; and Leite, N. 2011. Text detection and recognition in urban scenes. In *2011 IEEE International Conference on Computer Vision Workshops (ICCV Workshops)*, 227–234. doi:10.1109/ICCVW.2011.6130247.
- Mishra, A.; Alahari, K.; and Jawahar, C. 2012. Scene Text Recognition using Higher Order Language Priors. In *Proceedings of the British Machine Vision Conference 2012*, 127.1–127.11. Surrey: British Machine Vision Association. ISBN 978-1-901725-46-9. doi:10.5244/C.26.127. URL <http://www.bmva.org/bmvc/2012/BMVC/paper127/index.html>.
- Neumann, L.; and Matas, J. 2012. Real-time scene text localization and recognition. volume 38, 3538–3545. ISBN 978-1-4673-1226-4. doi:10.1109/CVPR.2012.6248097.
- Pan, Y.-F.; Hou, X.; and Liu, C.-L. 2011. A Hybrid Approach to Detect and Localize Texts in Natural Scene Images. *IEEE Transactions on Image Processing* 20(3): 800–813. ISSN 1941-0042. doi:10.1109/TIP.2010.2070803. Conference Name: IEEE Transactions on Image Processing.
- Petrova, O.; and Bulatov, K. 2019. Methods of machine-readable zone recognition results post-processing. In *Eleventh International Conference on Machine Vision (ICMV 2018)*, volume 11041, 110411H. International Society for Optics and Photonics. doi:10.1117/12.2522792. URL <https://www.spiedigitallibrary.org/conference-proceedings-of-spie/11041/110411H/Methods-of-machine-readable-zone-recognition-results-post-processing/10.1117/12.2522792.short>.
- Ren, S.; He, K.; Girshick, R.; and Sun, J. 2015. Faster r-cnn: Towards real-time object detection with region proposal networks. In *Advances in neural information processing systems*, 91–99.
- Sandler, M.; Howard, A.; Zhu, M.; Zhmoginov, A.; and Chen, L.-C. 2018. MobileNetV2: Inverted Residuals and Linear Bottlenecks. *2018 IEEE/CVF Conference on Computer Vision and Pattern Recognition* doi:10.1109/cvpr.

2018.00474. URL <http://dx.doi.org/10.1109/CVPR.2018.00474>.

Sermanet, P.; Eigen, D.; Zhang, X.; Mathieu, M.; Fergus, R.; and LeCun, Y. 2013. OverFeat: Integrated Recognition, Localization and Detection using Convolutional Networks.

Shi, B.; Bai, X.; and Belongie, S. 2017. Detecting Oriented Text in Natural Images by Linking Segments. *arXiv:1703.06520 [cs]* URL <http://arxiv.org/abs/1703.06520>. ArXiv: 1703.06520.

Simonyan, K.; and Zisserman, A. 2014. Very Deep Convolutional Networks for Large-Scale Image Recognition.

Smith, R. 2007. An overview of the Tesseract OCR engine. In *Ninth international conference on document analysis and recognition (ICDAR 2007)*, volume 2, 629–633. IEEE.

Tretyakov, K. 2016. PassportEye: Extraction of machine-readable zone information from passports, visas and id-cards via OCR. URL <https://github.com/konstantint/PassportEye>.

Wang, J.; and Hu, X. 2017. Gated recurrent convolution neural network for ocr. In *Advances in Neural Information Processing Systems*, 335–344.

Wang, W.; Xie, E.; Li, X.; Hou, W.; Lu, T.; Yu, G.; and Shao, S. 2019. Shape Robust Text Detection with Progressive Scale Expansion Network. *arXiv:1903.12473 [cs]* URL <http://arxiv.org/abs/1903.12473>. ArXiv: 1903.12473.

Xie, E.; Zang, Y.; Shao, S.; Yu, G.; Yao, C.; and Li, G. 2018. Scene Text Detection with Supervised Pyramid Context Network. *arXiv:1811.08605 [cs]* URL <http://arxiv.org/abs/1811.08605>. ArXiv: 1811.08605.

Xing, L.; Tian, Z.; Huang, W.; and Scott, M. R. 2019. Convolutional Character Networks. *arXiv:1910.07954 [cs]* URL <http://arxiv.org/abs/1910.07954>. ArXiv: 1910.07954.

Xu, Y.; Duan, J.; Kuang, Z.; Yue, X.; Sun, H.; Guan, Y.; and Zhang, W. 2019. Geometry Normalization Networks for Accurate Scene Text Detection. *arXiv:1909.00794 [cs]* URL <http://arxiv.org/abs/1909.00794>. ArXiv: 1909.00794.

Zhang, Z.; Zhang, C.; Shen, W.; Yao, C.; Liu, W.; and Bai, X. 2016. Multi-Oriented Text Detection with Fully Convolutional Networks. *arXiv:1604.04018 [cs]* URL <http://arxiv.org/abs/1604.04018>. ArXiv: 1604.04018.

Zhou, X.; Yao, C.; Wen, H.; Wang, Y.; Zhou, S.; He, W.; and Liang, J. 2017. EAST: An Efficient and Accurate Scene Text Detector. *arXiv:1704.03155 [cs]* URL <http://arxiv.org/abs/1704.03155>. ArXiv: 1704.03155 version: 2.

Zhu, K.-h.; Qi, F.-h.; Jiang, R.-j.; and Xu, L. 2007. Automatic character detection and segmentation in natural scene images. *Journal of Zhejiang University: Science A* 8: 63–71. doi:10.1631/jzus.2007.A0063.